ISSN 2278-3091
Volume 9 No.2, March - April 2020
International Journal of Advanced Trends in Computer Science and Engineering
Available Online at http://www.warse.org/IJATCSE/static/pdf/file/ijatcse126922020.pdf
https://doi.org/10.30534/ijatcse/2020/126922020

Performance Analysis of Polar Codes and LDPC Codes in Optical Satellite Communication Systems

Thong D. Nguyen[1], Binh A. Nguyen[2], Viet Q. Tran[2], Manh Hoang[2],Nhan D. Nguyen[3], Giao N. Pham[4], Yong-il Park[5]

[1]Thong D. Nguyen, Faculty of Eng., & Tech., QuyNhon University, Vietnam, thongnguyenduy88@gmail.com
[2]ICT Department, FPT University, Hanoi, Vietnam, binhnase04865@fpt.edu.vn, viettqse06178@fpt.edu.vn, manhhhe130294@fpt.edu.vn
[3]Dept. of Biomedical Engineering, Sungkyunkwan University, Suwon, South Korea, nhannd@skku.edu
[4]Dept. of Computing Fundamentals, FPT University, Hanoi, Vietnam, giaopn@fe.edu.vn
[5]Youngil Park, Dept. of Electronics Engineering, Kookmin University, South Korea, ypark@kookmin.ac.kr

ABSTRACT

In recent years, the demand for high data rate services has increased dramatically. Meanwhile, traditional radio communication is overloaded due to limited bandwidth and channel capacity. With broad-spectrum, optical wireless communications using a laser is considered as a promising solution for providing ultra-fast data rate for satellite communication systems. However, the fading caused by atmospheric turbulence is one of the most reasons to degrade the system performance of satellite communication. Therefore, a robust channel coding is required to maintain the stable transmission, such as low-density parity check (LDPC) code or Polar code. In this research, the satellite environment channel is reproduced in aiming to simulate the fading noise caused by atmospheric turbulence. Next, the performance of the LDPC codes and Polar codes is evaluated in different channel environments. However, the conventional form of both codes cannot overcome the fading noise due to atmospheric turbulence. Therefore, interleaving is applied to enhance the system performance further and reduce the computation time. Simulation results show that the scheme of block-interleaving and LDPC codes is more efficient compared to that of the Polar scheme. The gain is 2 dB at the BER of 10-3. The computation time of LDPC scheme is reduced significantly as interleaving is employed, while that of Polar scheme is stable with varying environments.

Key words: Polar codes, Low-density parity check codes, optical wireless communications, optical satellite communication, interleaving

1. INTRODUCTION

In recent years, communications based on a laser have become interesting research due to the high data rate and unlimited bandwidth. In recent researches, the laser has emerged as a new means to send data to the satellite due to the overloading of RF technologies. However, in order to deploy optical in the satellite communication systems, many issues need to be resolved, such as distance transmission, atmospheric turbulence, and abnormal weather conditions. For these reasons, the light intensity of the received signal is severely degraded and then reducing the system performance. This problem can be mitigated by increasing the laser power; however, the power supply of the satellite is always limited. Therefore, an effective coding scheme will be an approach to overcome atmospheric turbulence and enhance system performance.

Like optical camera communication system [1]-[3], optical satellite communication system (OSC) is also light-of-sight system. The transmitter and the receiver must see each other for communication. Thus, any sort of obstacle (e.g., cloud, bird, rain, snow, etc) between them causes the error. Consequently, a lot of bits will be lost in a short period. The higher the data rate, the larger the size of the burst error. For instance, 1 Mbit data will be lost within 10 ms if the data rate is 100 Mbps. A conventional error correction codes (ECC) is not suitable for overcoming the large size of burst error, which is up to a thousand bits. In recent years, LDPC is an attractive subject in both fields of academia and industry [4]-[6]. Its performance can reach the Shannon limit, differs by only 0.0045 dB, as demonstrated in [7]. LDPC codes have utilized in many wireless standards, such as digital video broadcast, IEEE 802.11, and the Advanced Television System Committee [8]. Besides, the performance of Polar codes was also proven to achieve the symmetric capacity of memory less channels [9] and low-complexity implementation. With the outstanding performance, LDPC codes and Polar codes were recommended as candidates for 5G New Radio [10], [11]. However, the conventional LDPC/Polar codes cannot guarantee a steady performance in the OSC; therefore, a combination with interleaving is proposed to improve the system performance in the tough environment.

The main purpose of the paper is to reproduce the fading noise caused by atmospheric turbulence. Next, the performance of LDPC codes and Polar codes are evaluated under the fading channel of OSC system. The performance of both codes is compared in the resistance of burst error. Once

block-interleaving is utilized, the performance and computation time are analyzed in aiming to select the proper codes for the OSC system.

2. SYSTEM ANALYSIS

2.1 Temporal Frequency Spectrum

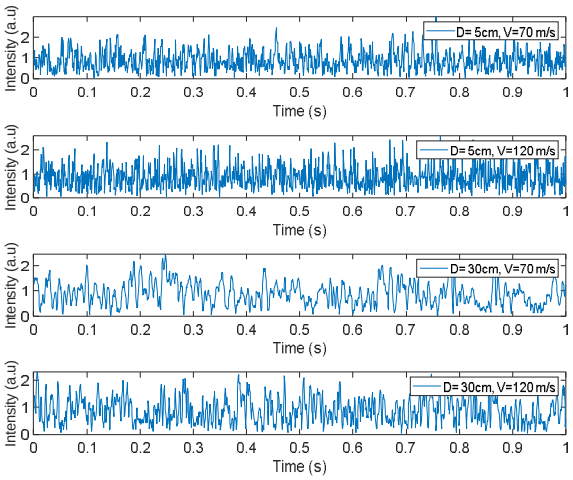

Figure 1: The simulated signals for different wind velocity and receiver diameter.

The power spectrum of atmospheric turbulence is involved with temperature, index of refraction and wind velocity. It is a function of the probability of frequencies, which are comprised in the received signal. In [12], the temporal power spectrum of atmospheric turbulence is expressed as (1)

$$W_e^2(f) = \frac{0.033C_n^2\tau_r^2D^2}{4V^2}\int_0^\infty \frac{J_1^2\left(\pi D\sqrt{\kappa^2+f^2/V^2}\right)}{\kappa^2+f^2/V^2} \times \frac{\exp\left[-\left(\kappa^2+f^2/V^2\right)/\kappa_m^2\right]}{\left(\kappa^2+f^2/V^2+\kappa_0^2\right)^{11/6}}d\kappa \quad (1)$$

In this equation, the profile model, $C_n^2(h)$, is used to indicate the varying strength of optical turbulence, which is a function of wind velocity V and altitude h. The Hufnagel-Valley (H-V) model [12], [13], one of the most widely used schemes, is utilized in this paper. Besides, J_1 is the Bessel function of the first kind, D is the receiver diameter, τ_r is an optical loss, κ is the spatial frequency vector, f is the frequency elements in the received signal, $\kappa_m = 5.92/l_0$, $\kappa_0 = 2\pi/\mathrm{L}_0$, l_0 is an inner scale and L_0 is an outer scale. Assuming that the altitudesof ground stations and satellites are constant. As a result, the temporal power spectrum is a function of the receiver diameter (D) and the wind velocity (V). To generate the random time-varying signal, next, the power spectral density (PSD) is expressed as following equation.

$$W_e'(f) = W_e(f)\times\exp\left[j\varphi(f)\right] \quad (2)$$

where $\varphi(f)$ is the random phase in [0, 2π]. Then, by using inverse fast Fourier transform, the time-varying signals can be generated, as in (3).

$$e(t) = \left|\Im^{-1}\left[W_e'(f)\right]\right| \quad (3)$$

Fig. 1 simulates the received signal in the time domain, which is acquired from (1) and (3), where l_0=4×10^{-3} m, L_0=1.6 m, and C_n^2= 1.4×10^{-18} m$^{-2/3}$ are calculated at the altitude of 20 km. From Fig. 1, it can be viewed that the fluctuation of the received signal is proportional to the wind velocity and inversely proportional to receiver diameter.

2.2 Low-Density Parity Check (LDPC) Codes

LDPC codes were first proposed by Gallager in his doctoral dissertation in the 1960s [14]. Like other block codes, LDPC codes are represented by a parity-check matrix H, which has a low density of 1's, as in Fig. 2(a). A Tanner graph represents the parity-check matrix in the form of a bipartite graph [15], where check nodes c are connected to the variable nodes v, as shown in Fig. 2(b). The check nodes and variable nodes are connected whenever the element in H matrix is a 1. The check nodes and variable nodes correspond to the rows and columns in the matrix H, respectively. The Tanner graph converted from the H matrix is illustrated in Fig. 2.

The data recovery function of LDPC codes against the burst error can be explained in Fig. 2. As shown in Fig. 2(b), since each variable node is linked to multiple check nodes at different positions, multiple check nodes will receive wrong information when only a variable node is wrong, as illustrated by the red line in Fig. 2(b). However, as a check node is linked to multiple variable nodes at the same time, the aggregated information is still reliable assuming that most of its connected variable nodes are valid. Then, the information from the check nodes is forwarded to variable nodes. Simultaneously, the information of other trusted nodes also supports the error nodes to retrieve the information. The decoding process is repeated many times until the number of iterations exceeds the given iterations, or all data is recovered completely. Therefore, system performance depends on the number of iterations or coding efficiency. A large-size LDPC block can achieve high performance but at the cost of complexity. Besides, the decoding algorithm also affects to system performance as well as complexity. The hard decision is simple and easy to implement, while the soft decision achieves higher performance. The LDPC codes with the hard decision are necessary for use against the white noise, while the soft decision is adopted to overcome the harsh environment. Therefore, the appropriate decoder type should be selected considering both the environment and the complexity.

2.3 Polar Codes

Like LDPC codes, Polar code is also a linear block error correction code, which was invented by ErdalArikan in 2009 [9]. They provide the first deterministic construction of capacity-approaching codes for binary memory less symmetric channels. The channel capacity can be acquired when the information bits are located in the reliable channels, while the frozen bits (i.e., usually zeros) are located in the unreliable channel. Polar codes can be specified by (K, N), where N is the number of the codeword bits (bit), K is the number of information bits (bit). The position of information bits is indicated in a set of K indices, $I \in \{0, 1, \ldots, N\}$, while the frozen bits indices are the complementary set I^c. The codeword x is generated as follows.

$$x = G\cdot u = F^{\otimes n}\cdot u \quad (4)$$

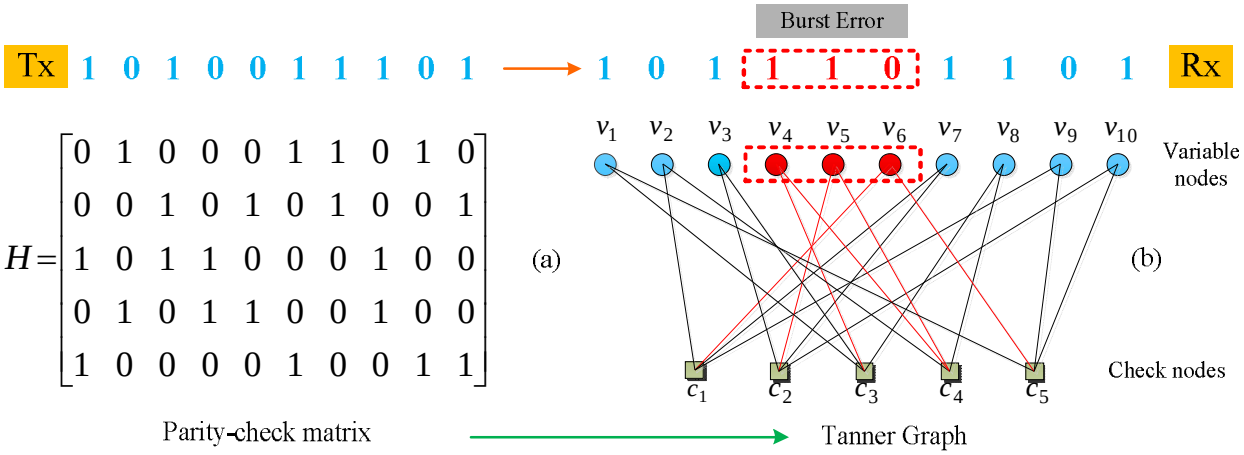

Figure 2: The LDPC codes, (a) The parity-check matrix, and (b) The Tanner graph.

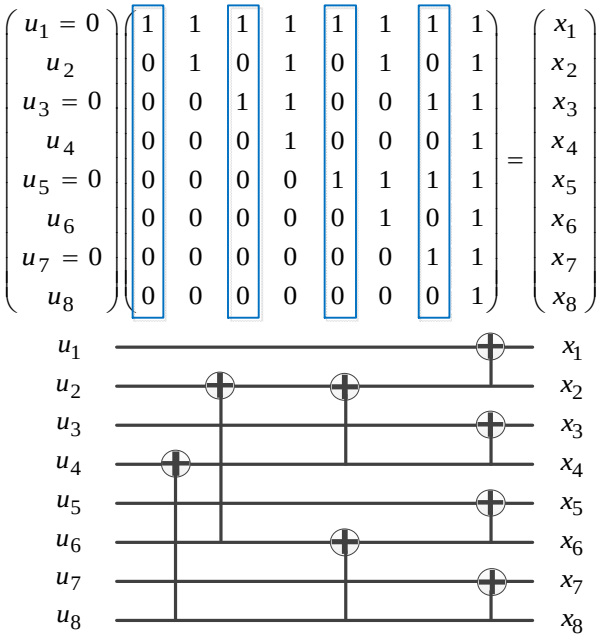

Figure 3. Construction of Polar encoder of length 8.

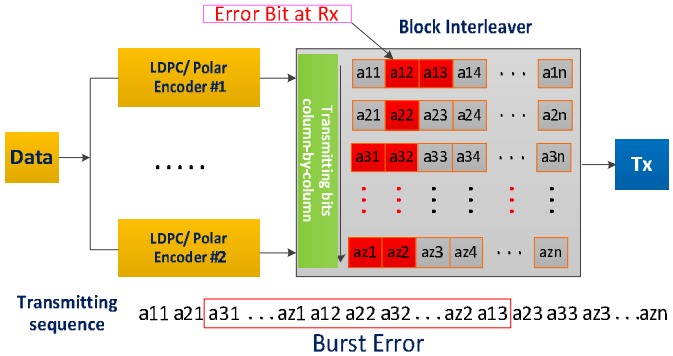

Figure 4: The diagram of block-interleaving.

$$F = \begin{bmatrix} 1 & 1 \\ 0 & 1 \end{bmatrix} \quad (5)$$

An example of the construction of Polar code (4, 8) is indicated in Fig. 3. In this paper, the successive cancellation decoder (SCD) algorithm is used for the decoder. It resembles the classic belief propagation algorithm, which is adopted for the LDPC decoder.

2.4 Interleaving

A serious issue of any light-of-sight system is the burst error. The fading caused by atmospheric turbulence, obstacles between the transmitter and the receiver are the reasons of the burst error in the OSC system. As a result, a lot of bits will be lost in a short period of time. For linear block codes, the severity of the burst error can be estimated by the number of the consecutive error bits. Polar codes and LDPC codes canacquire a high performance against white noise. However, a burst error cannot be solved by short block code, while a large one increases the complexity. Therefore, a combination of linear codes and block interleaving is proposed. A block interleaving will include multiple short blocks of Polar codes or LDPC codes. In this scheme, the data of the interleaved block is transmitted intermittently in column order. Therefore, the burst error will disperse across many short blocks if error occurs. As a result, each short block comprises only a few errors, and the data is retrieved easily. In Fig. 4, an interleaved block included z-blocks is illustrated. The performance of the system is directly proportional to the block size. However, it is inversely proportional to the processing time, since the receiver must wait until the whole data of the interleaved block is received.

3. PERFORMANCE ANALYSIS

In this section, the performance of LDPC codes and Polar codes are tested under the atmospheric turbulence environment of the OSC system. Besides, the complexity of both codes is also evaluated based on computation time, which is the most important parameter when deploying the real system in practice. The parameters utilized for all simulations are listed in Table I.

Table 1: Classification accuracy of features each MET level.

Parameters		Value
LDPC codes	Size	(324,648), (2592,5184)
	Code rate	0.5
	Iteration	30
	Algorithm	Sum-product algorithm
Polar codes	Size	(512,1024), (8192,16384)
	Code rate	0.5
	Frozen bit	0
	Algorithm	Successive cancellation decoder
Modulation		On-Off Keying
Data rate		1.134 Mbps
Wind velocity		70 m/s
Number of transmitted bits		106 bits
Receiver diameter		30 cm
Structure parameter C_n^2		1.4e-18 m-2/3
Satellite attitude		20 km
Ground station attitude		100 m
Inner scale		4 mm
Outer scale		1.6 m

In most previous papers, the performance of both codes was evaluated under AWGN channel. The performance comparison between LDPC codes and Polar codes is shown in [16]-[18], where LDPC codes can achieve high performance compared to Polar codes with the short packet. Both codes obtain the same performance as the length of Polar block is long enough. In the OSC system, however, the burst error happens frequently and it's more serious in the harsh environment. Therefore, this paper only focuses on evaluating the performance of both codes under atmospheric turbulence, which causes the burst error in the OSC system.

As above mentioned, fluctuation of the received signal is caused by wind velocities and diameters, which affect the system performance directly. The wind velocity of 70 m/s and the receiver diameter of 30 cm are used for all simulations in this paper. In Fig. 5, the conventional Polar codes and LDPC codes did not show the efficiency. The performance of Polar (512, 1024) is equal to that of the un-coded scheme. The performance of Polar (8192, 16384) is worst even a long code length was used. While the performance of LDPC 648 is also not outstanding compared to that of Polar codes. The low performance is attributed to the burst error. From the simulation results in Fig. 5, it can be concluded that a conventional ECC is not suitable for the OSC system. Therefore, interleaving can be a solution to this issue.

In Fig. 6, it can be observed that a long block of Polar code is not effective in the OSC system. However, the performance of the long Polar block is improved significantly as interleaving is used. The simulation results in Fig. 6 show that this method is only effective with a long block of Polar codes. In contrast, the performance of LDPC (2592, 5184) shows a better performance compared to Polar codes. The gain of 1 dB is shown at the Bit Error Rate of 10-3 even it has short code length compared to that of Polar codes.

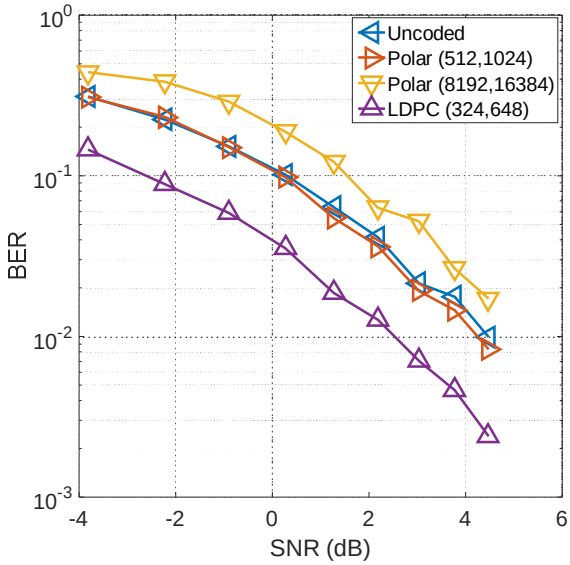

Figure 5: Performance of LDPC codes and Polar codes in the OSC system.

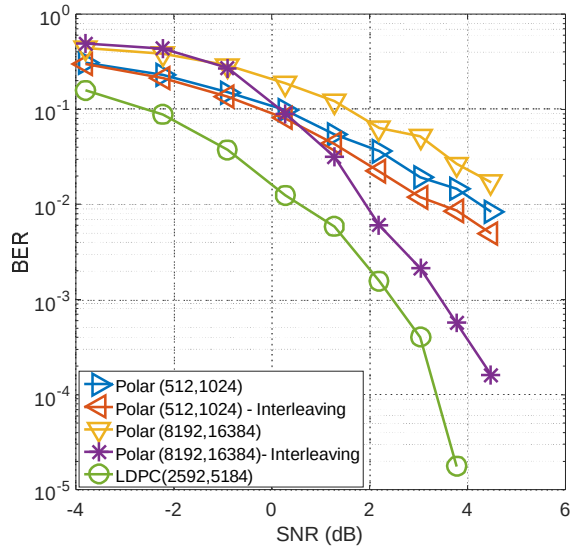

Figure 6: Performance comparison between LDPC codes and Polar codes combined interleaving

A short block cannot achieve high performance while the longer one requires more computation time. Therefore, the next simulation will combine multiple short blocks of LDPC/Polar codes in an interleaving block. It is expected to obtain high performance and reduce computation time. As indicated in Fig. 7, with the same length, the performance of Polar (8192, 16384) and 8-interleaved blocks Polar (512, 1024) is nearly the same. The performance of Polar is enhanced further as the number of Polar blocks is increased. However, the performance of Polar codes is still lower than that of 32-interleaved blocks LDPC (324,648), even the length of Polar interleaved block is nearly 4 times compared to that of LDPC interleaved block. Compared to Polar codes, the differences are 1 dB and 2 dB when 32 and 64 interleaved-blocks of LDPC 648 are used, respectively.

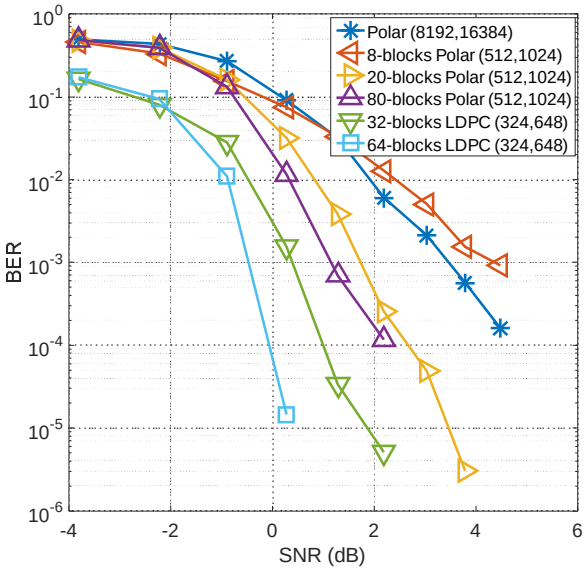

Figure 7: Performance of interleaved Polar/LDPC codes.

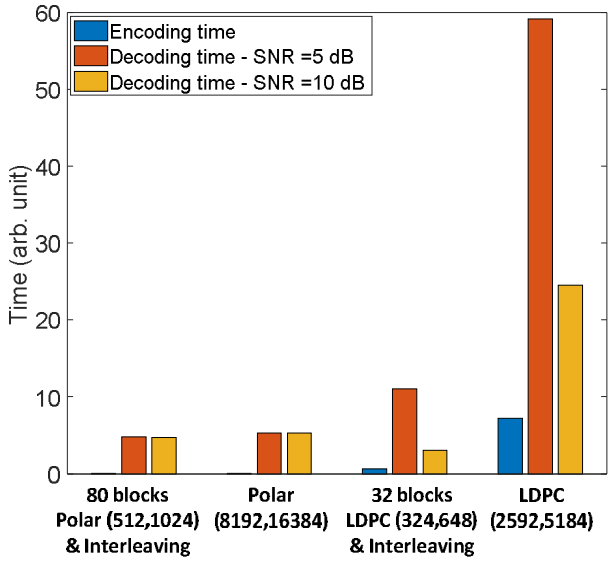

Figure 8: The computation time of the different coding scheme.

In the next simulation, more than 81,000 bits are tested. The computation time between Polar codes and LDPC codes are compared. The simulation result in Fig. 8 shows that the encoding time of Polar codes is very small compared to that of the LDPC codes. Moreover, the big difference can be shown as the length of the LDPC codes is increased. The decoding time of Polar codes is stable in varying environments. In contrast, the decoding time of LDPC codes depends on the environment. Furthermore, the computation time is increased as the block length is extended. Reducing the number of iteration can reduce the computation time of LDPC codes, but at the cost of performance.

4. CONCLUSION

In this work, the fading noise due to atmospheric turbulence is reproduced by using the PSD of an optical satellite channel. The performance of LDPC codes and Polar codes are evaluated in the OSC system. The conventional Polar codes achieve a low performance compared to that of LDPC codes. The performance of Polar codes is improved as interleaving is applied. However, it still lower than LDPC scheme without interleaving. Both codes achieve high performance as the size of the interleaving block is extended. The gain of 2 dB is shown as the performance of 64-interleaved blocks LPDC 648 and 80-interleaved blocks Polar 1024 are compared. The processing time of large LDPC block is much longer than that of Polar codes. However, it is reduced as interleaving is used.

ACKNOWLEDGEMENT

This work was supported by the FPT University, Ha Noi, Vietnam, and QuyNhon University, BinhDinh, Vietnam. It is also supported by the Sungkyunkwan University, Kookmin University, Seoul, South Korea.

REFERENCES

1. D. T. Nguyen, Y. Chae, Y. Park. **Enhancement of Data Rate and Packet Size in Image Sensor Communications by Employing Constant Power 4-PAM**, IEEE Access, Vol. 9, pp. 8000-8010, Feb. 2018. https://doi.org/10.1109/ACCESS.2018.2802948
2. D. T. Nguyen, Y. Park. **Data rate enhancement of optical camera communications by compensating inter-frame gaps**, Optics Communications, Vol. 394, pp. 56–61, July. 2017.
3. D. T. Nguyen, S. Park, Y. Chae and Y. Park. **VLC/OCC Hybrid Optical Wireless Systems for Versatile Indoor Applications**, in IEEE Access, Vol. 7, pp. 22371-22376, 2019. https://doi.org/10.1109/ACCESS.2019.2898423
4. D. Mackay. **Good error correcting codes based on very sparse matrices**, in Cryptography and Coding, 5th IMA Conf., C. Boyd, Ed., Lecture Notes in Computer Science, pp. 100-111, 1995.
5. T. J. Richardson, and R. Urbanke. **Efficient Encoding of Low-Density Parity Check Codes**," IEEE Trans. Information Theory, Vol. 47, pp. 638-656, Feb. 2001. https://doi.org/10.1109/18.910579
6. Brian K. Butler. **Minimum Distances of the QC-LDPC Codes in IEEE 802 Communication Standards**, IEEE ISIT 2016, Feb. 2016.
7. S. Y. Chung, G. D. Forney, T.J. Richardson, R. Urbanke. **On the design of low-density parity-check codes within 0.0045 dB of the Shannon Limit**, IEEE Communications Letter, pp. 58–60, 2001. https://doi.org/10.1109/4234.905935
8. "IEEE 802.11n/ac/ax (WiFi) LDPC Decoder and Encoder,"Available: https://www.creonic.com/en/ip-core/ieee-802-11n-ac-wi fi-ldpc-decoder/, accessed on 13 April 2020.
9. E. Arikan. **Channel Polarization: A Method for Constructing Capacity-Achieving Codes for Symmetric Binary-Input Memoryless Channels**, IEEE

Transactions on Information Theory, Vol. 55, No. 7, pp. 3051-3073, July 2009.
10. T. Richardson and S. Kudekar. **Design of Low-Density Parity Check Codes for 5G New Radio**, IEEE Communications Magazine, Vol. 56, No. 3, pp. 28–34, Mar 2018.
11. Chairman's Notes Agenda Item 7.1.5 Channel Coding Modulation. Available: http://www.3gpp.org/ftp/tsg_ran/WG1_RL1/TSGR1_87/Docs/R1-1613710.zip, accessed on 13 April 2020.
12. Larry C. Andrews, Ronal L. Phillips. **Laser Beam Propagation through Random Media**, SPIE Press, Chap. 3, pp. 57-82, Sep. 2005. https://doi.org/10.1117/3.626196
13. M. Toyoshima, H. Takenaka, Y. Takayama. **Atmospheric Turbulence-Induced Fading Channel Model for Space-to-Ground Laser Communications Links**, Optics Express, vol. 19, no. 17, Aug. 2011.
14. R. Gallager. **Low-Density Parity Check Codes**, IRE Trans. Information Theory, pp. 21–28. Jan. 1962.
15. R. Tanner. **A Recursive Approach to Low Complexity Codes**," in IEEE Transactions on Information Theory, Vol. 27, No. 5, pp. 533–547, Sep. 1981. https://doi.org/10.1109/TIT.1981.1056404
16. G. Sarkis, P. Giard, A. Vardy, C. Thibeault and W. J. Gross. **Fast Polar Decoders: Algorithm and Implementation**, IEEE Journal on Selected Areas in Communications, Vol. 32, No. 5, pp. 946-957, May 2014.
17. M. Noor, R. Amir, A. Mohamad, and M. Amin. **CNDS-Rules and Pattern Based Signal Recovery for Multi-level Signal Decision Making**, International Journal of Advanced Trends in Computer Science and Engineering, Vol. 8, No. 4, pp. 356-362, 2019. https://doi.org/10.30534/ijatcse/2019/5481.42019
18. A. A. Mohammed, A. Z. Mohammed. **Multilayer Neural Network based on MIMO and Channel Estimation for Impulsive Noise Environment in Mobile Wireless Networks**, International Journal of Advanced Trends in Computer Science and Engineering, Vol. 9, No. 1, pp. 315-321, 2020. https://doi.org/10.30534/ijatcse/2020/48912020